Investigation of dielectric relaxation processes in Ba2NdFeNb4-xTaxO15 ceramics

Martynas Kinka, D. Gabrielaitis, Marjorie Albino, Michaël Josse, E. Palaimiene, Robertas Grigalaitis, Mario Maglione, Juras Banys

Investigation of Dielectric Relaxation Processes in $Ba_2NdFeNb_{4-x}Ta_xO_{15}$ Ceramics

M. KINKA,[1] D. GABRIELAITIS,[1] M. ALBINO,[2] M. JOSSE,[2] E. PALAIMIENE,[1,*] R. GRIGALAITIS,[1] M. MAGLIONE,[2] AND J. BANYS[1]

[1]Vilnius University, Faculty of Physics, Lithuania
[2]CNRS, Université de Bordeaux, ICMCB-CNRS, France

Dielectric response of $Ba_2NdFeNb_{4-x}Ta_xO_{15}$ (x 0.3, 0.6 and 2) solid solutions with Tetragonal Tungsten Bronze structure has been investigated by means of broadband dielectric spectroscopy in the frequency range from 20 Hz to 37 GHz. Pure $Ba_2NdFeNb_4O_{15}$ compound displays ferroelectric behavior. Substitution of Nb^{5+} by Ta^{5+} considerably alters dielectric response of this system. Ferroelectric state was observed only for x 0.3 compound with slightly lowered ferroelectric phase transition temperature. Further increase of x causes formation of relaxor state in these solid solutions and considerably lowers corresponding dielectric permittivity dispersion temperature region.

Keywords: Tetragonal tungsten bronze; broadband dielectric spectrosopy; ferroelec trics; ferroelectric relaxor; dielectric relaxation

Introduction

$Ba_2NdFeNb_{4-x}Ta_xO_{15}$ ceramics under investigation here belong to the tetragonal tungsten bronze (TTB) structural family, which attracted much attention in recent years. It is one of the largest oxygen octahedral ferroelectric families next to the ferroelectric perovskites [1]. A wide range of substitutions is available in TTB framework, which makes it a promising candidate in search of relaxors, ferroelectrics and even multiferroics. Three types of open channels (pentagonal A1, square A2, trigonal C) that develop within its octahedral framework can be occupied by cations, which results in general formula $A1_2A2_4C_4(B1_2, B2_8)O_{30}$ [2], [3]. In $Ba_2NdFeNb_{4-x}Ta_xO_{15}$ the octahedral framework is statistically occupied by Fe^{3+}, Nb^{5+} and Ta^{5+} cations, while Ba^{2+} cations are located inside pentagonal and Nd^{3+} inside square channels.

$Ba_2LnFeNb_4O_{15}$ (Ln = La, Pr, Nd, Sm, Eu, Gd) family of ceramics is known to have a variety of interesting properties. Compounds with neodymium, samarium and europium are ferroelectrics, while ceramics with praseodymium and gadolinium exhibit relaxor properties [4,5]. Moreover, Pr, Nd, Sm, Eu, Gd samples exhibit a room temperature magnetic hysteresis loops [5]. Pure $Ba_2NdFeNb_4O_{15}$ compound exhibits anomalous behavior of dielectric permittivity associated with ferroelectric phase transition, which is accompanied by unusually wide thermal hysteresis [4]. A wide thermal hysteresis most likely is a

common feature among all $Ba_2LnFeNb_4O_{15}$ family ferroelectrics (Ln = Nd, Sm, Eu). It was also reported for a few other compounds with tetragonal tungsten bronze structure. For example, $Ba_4Ln_2Ti_4Nb_6O_{30}$ (Ln = Nd and Sm) and $Sr_4Ln_2Ti_4Nb_6O_{30}$ (Ln = Sm and Eu) ceramics, which exhibit ferroelectric properties and a similar dielectric permittivity evolution, while heating and cooling [6,7]. Processes observed in these two systems are attributed to the complex nature of the tetragonal tungsten bronze structure. Firstly it is a nonrandom distribution of two ferroelectrically active cations (Ti^{5+} ir Nb^{5+}) over two sets of sites, which may form more than one kind of polar cluster, and secondly a weak superstructure that changes from incommensurate to commensurate on cooling through T_c [6 8]. $Ba_4Ln_2Ti_4Nb_6O_{30}$ and $Sr_4Ln_2Ti_4Nb_6O_{30}$ systems can also exhibit a relaxor like dielectric response. This was achieved with La^{3+} content substitution in the square channels [9,10]. $Ba_2Pr_xNd_{x-1}FeNb_4O_{15}$ family again shows a continuous transition from ferroelectric to relaxor like behavior with increasing Pr amount [4]. Many of the observed phenomena are strongly dependent on the ion radius of A2 (square) sites. Substitutions within $Ba_2LnFeNb_4O_{15}$ (Ln = La, Pr, Nd, Sm, Eu, Gd) framework illustrate this very well. The ionic radius of lanthanides ions is known to decrease with increasing atomic number. Therefore, the evolution of the ferroelectric properties in the Nd, Sm and Eu compounds is as follows. The smaller the rare earth element is, the greater distortion of the TTB framework occurs. Consequently greater distortions of the TTB framework lead to greater permittivity and higher Curie temperatures [5]. Similar effects of rare earth elements in A2 site that determine dielectric behavior can be seen in many other TTB systems i.e., $Ba_2LnTi_2Nb_3O_{15}$ (Ln = Bi, La, Nd, Sm, Gd), $Ba_2(La_xNd_{1-x})Ti_2Nb_3O_{15}$. Here the classical ferroelectric behavior is controlled by a commensurate octahedral tilting, whose driving force increases as the average ionic radius of the A2 site ion decreases [11 13]. Other authors state that both ion radiuses of A1 and A2 sites are important, but the difference of the ionic radiuses ΔR plays the crucial role. ΔR is usually presented as the main parameter governing dielectric nature of filled tungsten bronzes [12 16]. Generally, the tungsten bronzes with larger ΔR indicate an obvious normal ferroelectric peak followed by some low temperature dielectric relaxations. With decreasing ΔR, the normal ferroelectric peak changes to the diffuse and relaxor ones gradually and the low-temperature dielectric relaxations become stronger [8,12 16].

In this paper we present our results on investigation of broadband dielectric properties of $Ba_2NdFeNb_{4-x}Ta_xO_{15}$ solid solutions (x = 0.3, 0.6, 2) concerning the substitution not at A2 sites, but within the octahedral framework. As this framework is usually considered as the origin of ferroelectricity in TTB niobates, it was expected that the substitution of Nb^{5+} ions by the ferroelectrically less active Ta^{5+} ions should have a significant effect on the dielectric properties of these ceramics.

Experimental Methods

$Ba_2NdFeNb_{4-x}Ta_xO_{15}$ ceramics (x = 0.3, 0.6, 2) have been obtained by a conventional solid state route. Powder x-ray diffraction showed a pure TTB phase for all compositions with a negligible addition of spurious phases. The compactness of all the studied samples was better than 92% as computed from density measurements. Dielectric measurements were performed on ceramic discs with deposited silver paste electrodes. The complex dielectric permittivity $\varepsilon^* = \varepsilon' - i\varepsilon''$ was measured using a capacitance bridge HP4284A in the frequency range 20 Hz 1 MHz, Agilent 8714ET RF vector network analyzer (VNA) at frequencies from 1 MHz to 3 GHz and scalar network analyzers by “Elmika” in the

8 GHz 37 GHz frequency range. Automatic temperature control setup was used to maintain a heating-cooling rate below 1 K/min.

Results and Discussion

Investigations of dielectric properties of $Ba_2NdFeNb_{3,7}Ta_{0,3}O_{15}$ ceramics have revealed two completely different responses on heating and cooling. Corresponding temperature dependencies of the real part of complex dielectric permittivity at selected frequencies are shown in Fig. 1. On heating two dielectric anomalies can be distinguished a diffuse one in the 150 K 200 K temperature range and well expressed peaks at 315 K. The latter temperature behavior of ε' has a characteristic form similar to that observed in pure $Ba_2NdFeNb_4O_{15}$ ceramics [4], where such peaks of dielectric permittivity with frequency independent position at 325 K have been associated with the ferroelectric phase transition. 10 K lower ferroelectric phase transition temperature in $Ba_2NdFeNb_{3,7}Ta_{0,3}O_{15}$ ceramics most likely is related to the introduction of Ta^{5+} cations, which also causes the

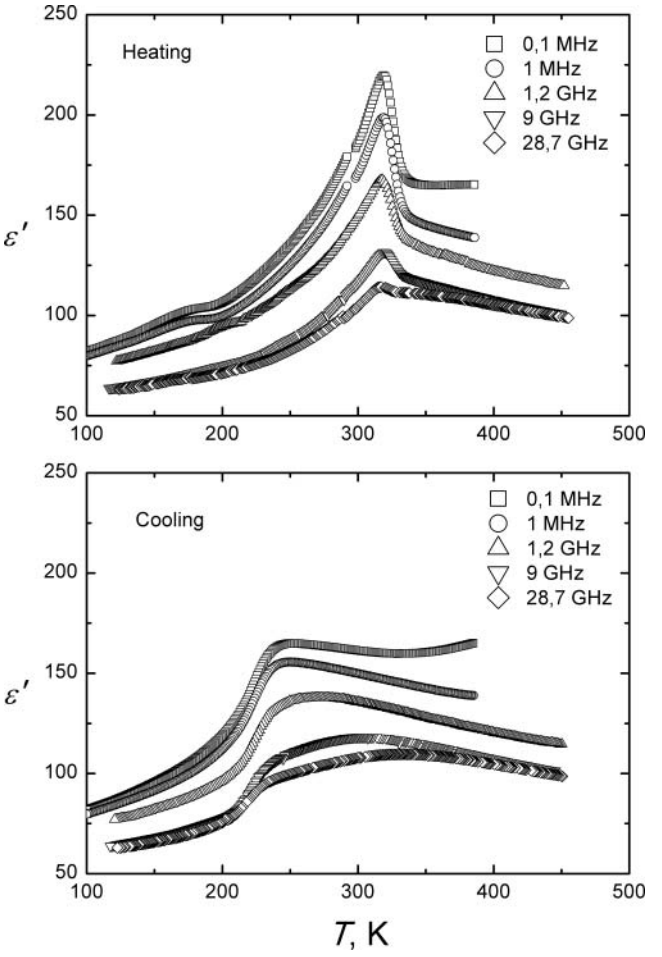

Figure 1. Temperature dependencies of the real part of complex dielectric permittivity of $Ba_2NdFeNb_{3,7}Ta_{0,3}O_{15}$ ceramic at different frequencies on heating and cooling.

appearance of additional low temperature dielectric dispersion region. On the following cooling run of dielectric measurements, a huge shift of permittivity maxima to lower temperatures (248 K) is observed. This lowering is accompanied with a complete change of the form of ε' temperature dependencies, which now obtain a diffuse shape, more characteristic to relaxors than to ferroelectric phase transition.

In order to elucidate such unusual temperature dielectric response of $Ba_2NdFeNb_{3,7}Ta_{0,3}O_{15}$ ceramics we have examined frequency dependencies of measured dielectric permittivity in a wide temperature range from 150 K to 360 K covering both dielectric anomalies. Characteristic frequency dependencies of the real and the imaginary parts of complex dielectric permittivity at selected temperatures are shown in Fig. 2. Similar forms of these dependencies were obtained on heating and cooling runs, where two relaxation processes (ii) and (iii) accompanied by the electrical conductivity region (i) at low frequencies can be distinguished. The best approximation results were obtained by using a superposition of two Cole-Cole equations with electrical conductivity term, which allowed us to estimate relaxation parameters for (ii) and (iii) processes:

$$\varepsilon^*(\omega) = \frac{\sigma^*}{i\varepsilon_0\omega^n} + \frac{\Delta\varepsilon_1}{1+(i\omega\tau_1)^{1-\alpha_1}} + \frac{\Delta\varepsilon_2}{1+(i\omega\tau_2)^{1-\alpha_2}} + \varepsilon_\infty, \qquad (1)$$

where ω is the angular frequency, n is a fit parameter, ε_∞ is the high frequency permittivity, $\Delta\varepsilon$ is the magnitude of the corresponding dispersion, τ is the corresponding relaxation time, α is the parameter that allows for the broadening of the dispersion, and σ is complex conductivity, reflecting the input of conductivity process.

Low frequency relaxation process (ii) is active within 1 kHz 100 MHz range. Its mean relaxation time is highly temperature dependent, as can be clearly seen from the imaginary part of complex dielectric permittivity. When temperature is rising from 150 K, a wide ε'' peak moves toward higher frequencies, however at 270 K this peak is no longer visible. It is hard to distinguish this process within the real part dependency due to electrical conductivity. The second, high frequency process (iii) is active within 0,1 GHz 12 GHz range. In this frequency region ε'' peaks are much narrower and their

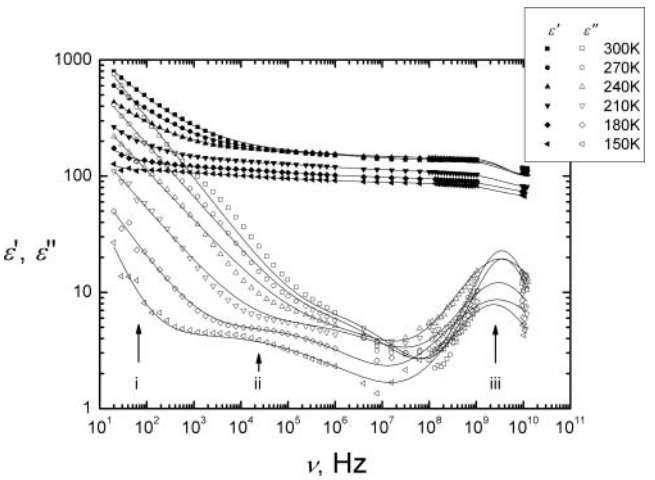

Figure 2. Frequency dependencies of the real and imaginary parts of complex dielectric permittiv ity of $Ba_2NdFeNb_{3,7}Ta_{0,3}O_{15}$ ceramic on cooling. Solid lines represent fits with 1 equation.

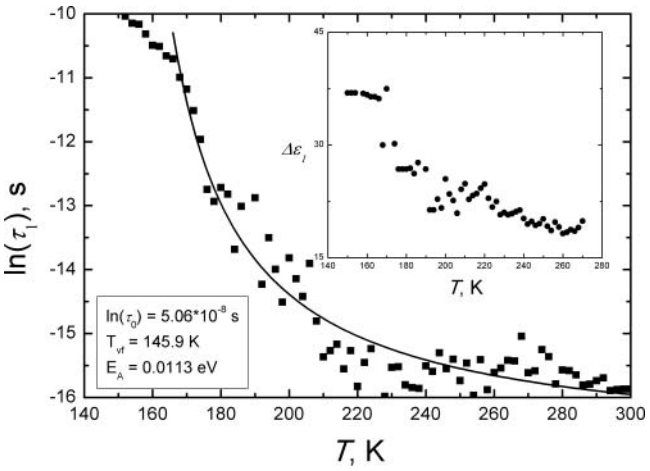

Figure 3. Temperature dependencies of the mean relaxation time $\ln(\tau_1)$ and relaxation strength $\Delta\varepsilon_1$ on cooling. $\ln(\tau_1)$ is approximated by Vogel Fulcher law.

position is less temperature dependent. Temperature dependency of the mean relaxation time $\ln(\tau_1)$ obtained from (1) on cooling run is shown in Fig. 3. It displays a rapid slowing down with decreasing temperature and can be well described by Vogel-Fulcher law with the following parameters: $T_{vf} = 145{,}9$ K and $E_A = 0{,}0113$ eV:

$$\tau = \tau_0 e^{\frac{E_A}{k(T - T_{vf})}}; \tag{2}$$

On heating a similar temperature behavior of $\ln(\tau_1)$ was observed with $T_{vf} = 146{,}2$ K and $E_A = 0{,}0111$ eV, confirming that this low frequency relaxation process (ii) has no heating cooling hysteresis. It gives a considerable contribution to the overall dielectric response of $Ba_2NdFeNb_{3,7}Ta_{0,3}O_{15}$ ceramics below ~240 K, but its relaxation strength (insert of Fig. 3) rapidly decreases with increasing temperature. Such dispersion features in the (ii) region indicate appearance of a separate, most likely relaxor, phase. Similar coexistence between relaxor and ferroelectric phases was reported for $Ba_2Pr_xNd_{1-X}FeNb_4O_{15}$ compound for $0<x<1$ [4]. Since pure $Ba_2NdFeNb_4O_{15}$ does not show relaxor behavior it is safe to assume that the appearance of this particular dispersion in $Ba_2NdFeNb_{3,7}Ta_{0,3}O_{15}$ compound is caused by the substitution of Nb by Ta cations, which leads to a higher chemical disorder. On the contrary, the higher frequency relaxation process (iii) parameter evolutions show a clearly pronounced heating cooling hysteresis (Fig. 4.). Estimated $\Delta\varepsilon_2$ temperature dependencies assemble a "butterfly" form. $\Delta\varepsilon_2(T)$ dependencies have peaks of almost the same height on heating and on cooling, which temperature positions coincide with ε' peaks in the measured dielectric response of $Ba_2NdFeNb_{3,7}Ta_{0,3}O_{15}$ ceramics (Fig. 1). Obtained temperature dependencies of the mean relaxation time τ_2 showed even more interesting behavior. On cooling $\tau_2(T)$ has a clear minimum around 290 K. It suggests that transition from paraelectric to ferroelectric state starts at higher temperatures than 237 K (where the maximum of $\Delta\varepsilon_2(T)$ is observed) and can explain the flattering of $\varepsilon'(T)$ peak in the GHz range (Fig. 1). On heating two minimums of $\tau_2(T)$ were found, indicating a complex mechanism of the phase transition in the 240 K 315 K temperature range. We can summarize at this point, that differences between overall dielectric response of $Ba_2NdFeNb_{3,7}Ta_{0,3}O_{15}$ solid solution on heating

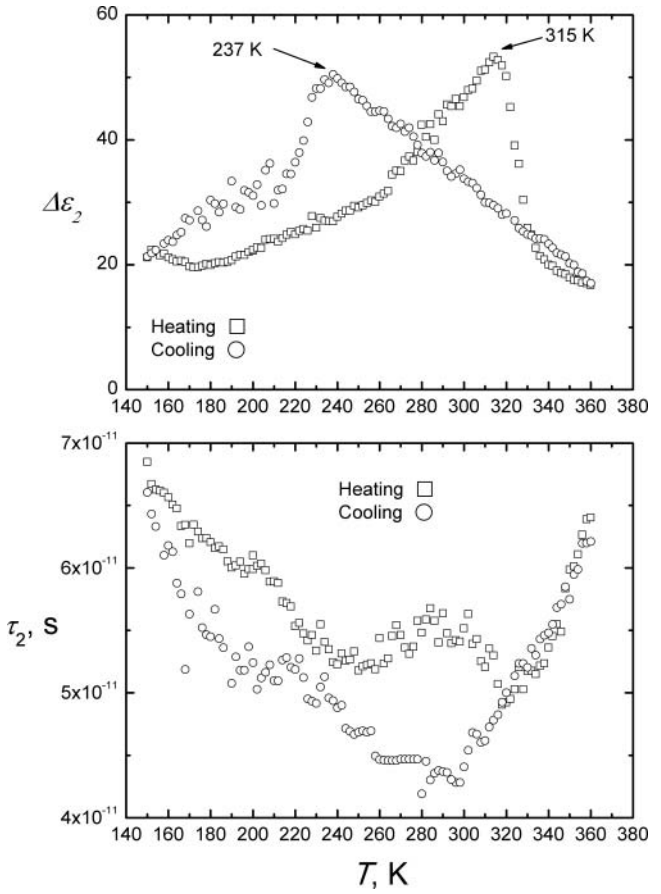

Figure 4. Temperature dependencies of relaxation strength $\Delta\varepsilon_2$ and the mean relaxation time $\ln(\tau_2)$ on cooling and heating.

and cooling (Fig. 1) are caused by the superposition and interaction of (ii) and (iii) relaxation processes. On cooling cycle, at 450 K the sample is in paraelectric phase. At this temperature (ii) process is inactive and has no impact on the sample properties. Situation starts to change only when 240 K 270 K temperatures are reached. As we stated earlier, low frequency process might be related to the ferroelectric relaxor state, therefore polar nanodomains might be forming at these temperatures. On the other hand, ferroelectric materials exhibit a long range ferroelectric order, while ferroelectric relaxors do not. Therefore, formation of polar nanodomains may be interrupting ferroelectric ordering, which leads to the broadening of ferroelectric phase transition on cooling. Below 240 K (ii) process becomes dominating, as the contribution of a high frequency process (iii) drops (Fig. 4). This leads to the overlapping dielectric dispersion in the 150 K 200 K temperature range as seen in Fig. 1. On heating we have a bit different situation, where both processes can be seen separately in the measured dielectric response. At low temperatures only the low frequency (ii) process is active. At 150 K 275 K its relaxation strength is decreasing rapidly, and later the (iii) process shows up ending with dielectric permittivity maxima at 315 K related to the phase transition in to the paraelectric phase.

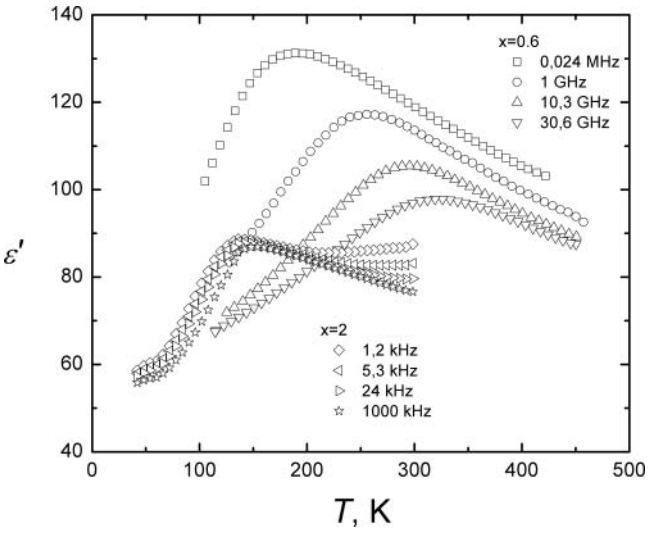

Figure 5. Temperature dependencies of the real part of complex dielectric permittivity of Ba_2Nd $FeNb_{4-x}Ta_xO_{15}$ ceramics with x 0.6 and x 2.

Investigations of $Ba_2NdFeNb_{3,4}Ta_{0,6}O_{15}$ (x = 0,6) sample with a higher concentration of tantalum showed that dielectric response completely changes its shape. Unlike for the previous sample (x = 0.3), here we do not see any heating cooling hysteresis. Also, no permittivity maxima or dispersion were found, which could be associated with ferroelectric phase transition. Variation of ε' and ε'' with temperature and frequency shows a "classical" example of a ferroelectric relaxor dielectric response [17]. Analysis of frequency dependencies of complex dielectric permittivity in a 20 Hz 36 GHz range at 300 K 150 K temperatures revealed one broad dielectric relaxation process, which mean relaxation time follows Vogel-Fulcher law. Further increase of Ta^{5+} content in

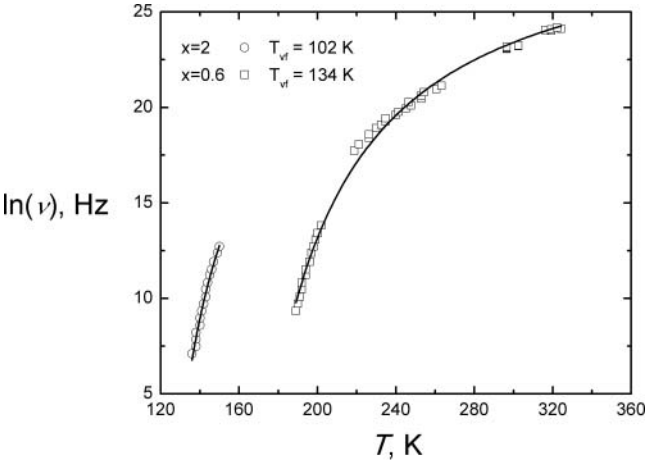

Figure 6. Temperature dependencies of dielectric permittivity maxima positions for Ba_2Nd $FeNb_{3,4}Ta_{0,6}O_{15}$ (x 0,6) and $Ba_2NdFeNb_2Ta_2O_{15}$ (x 2) ceramics, fitted with Vogel Fulcher equation.

$Ba_2NdFeNb_{4-x}Ta_xO_{15}$ structure shifts dielectric dispersion region towards lower temperatures [Fig. 5]. Again, observed temperature dependencies of the real and the imaginary parts of dielectric permittivity have a typical ferroelectric relaxor form. Our experimental setup was limited to 1 MHz at low temperatures, so we were unable to define relaxation parameters for this process. Instead temperature dependencies of dielectric permittivity maxima positions were determined, which both for $Ba_2NdFeNb_{3,4}Ta_{0,6}O_{15}$ (x = 0,6) and $Ba_2NdFeNb_2Ta_2O_{15}$ (x = 2) ceramics follow Vogel-Fulcher equation [Fig. 6], indicating a considerable shift of T_{vf} with increasing x.

Conclusions

Dielectric response of $Ba_2NdFeNb_{3,7}Ta_{0,3}O_{15}$ solid solution exhibits features of ferroelectric and ferroelectric relaxor states. Similar possible coexistence was reported for $Ba_2Pr_xNd_{1-X}FeNb_4O_{15}$ compounds [4], were relaxor properties were induced by rare earth ion substitutions at A2 sites. Introduction of Ta^{5+} cations within the octahedral framework also causes the appearance of relaxor like dielectric dispersion region in these TTBs and pushes ferroelectric phase transition to slightly lower temperatures. Despite these differences, cationic substitutions inside square channels and octahedral framework of these TTBs yield qualitatively to the same kind of dielectric behavior ferroeletric to relaxor crossover. Since Ta^{5+} replaces ferroelectrically active Nb^{5+} cations and introduces additional disorder in these systems, it enables relaxor state expression in $Ba_2NdFeNb_{4-x}Ta_xO_{15}$ solid solutions by suppressing ferroelectric state. With increasing Ta^{5+} concentration the complete vanishing of ferroelectric state was observed together with considerable lowering of relaxor dispersion region temperatures.

Funding

This research is funded by the European Social Fund under the Global Grant measure (project VP1-3.1-SMM-07-K-03-011).

References

1. B. A. Strukov, and A. P. Levanyuk, *Ferroelectric phenomena in crystals*. Germany: Springer Vergal; (1998).
2. P. B. Jamieson, S. C. Abrahams, and J. L. Bernstein, Ferroelectric Tungsten Bronze Type Crys tal Structures. I. Barium Strontium Niobate $Ba_{0.27}Sr_{0.75}Nb_2O_{5.78}$. *J Chem Phys.* **48**, 5048, (1968).
3. P. B. Jamieson, S. C. Abrahams, and J. L. Bernstein, Ferroelectric Tungsten Bronze Type Crys tal Structures. II. Barium Sodium Niobate $Ba_{(4+x)}Na_{(2-2x)}Nb_{10}O_{30}$. *J Chem Phys.* **50**, 4352, (1969).
4. J. Banys, S. Bagdzevicius, M. Kinka, V. Samulionis, R. Grigalaitis, E. Castel, M. Josse, and M. Maglione, Dielectric Studies Of $Ba_2Pr_xNd_{1-X}FeNb_4O_{15}$ Ceramics. Applications of Ferroelec trics (ISAF/PFM). 2011 International Symposium on Piezoresponse Force Microscopy and Nano scale Phenomena in Polar Materials; 1 3, (2011).
5. M. Josse, O. Bidault, F. Roulland, E. Castel, A. Simon, D. Michau, R. Von der Muhll, O. Nguyen, and M. Maglione, The $Ba_2LnFeNb_4O_{15}$ "Tetragonal Tungsten Bronze": Towards RT composite multiferroics. *Solid State Sci.* **11**, 1118 1123, (2009).
6. M. Prades, H. Beltrán, N. Masó, E. Cordoncillo, and A. R. West, Phase transition Hysteresis and Anomalous Curie Weiss Behaviour of Ferroelectric Tetragonal Tungsten Bronzes Ba_2RE $Ti_2Nb_3O_{15}$: RE Nd, Sm. *J. Appl. Phys.* **104**, 104118, (2008).

7. X. L. Zhu, and X. M. Chen, Thermal hysteresis of ferroelectric transition in $Sr_4R_2Ti_4Nb_6O_{30}$ (R Sm and Eu) tetragonal tungsten bronzes. *Appl. Phys. Lett.* **96**, 032901, (2010).
8. X. L. Zhu, and X. M. Chen, Phase transition hysteresis of ferroelectric $Sr_5EuTi_3Nb_7O_{30}$ ceramics with tetragonal tungsten bronze structure. *J. Appl. Phys.* **111**, 044104, (2012).
9. X. L. Zhu, K. Li, M. A. Rafiq, X. Q. Liu, and X. M. Chen, Relaxor nature in lead free Sr_5La $Ti_3Nb_7O_{30}$ tetragonal tungsten bronze ceramics. *J. Appl. Phys.* **114**, 124102, (2013).
10. K. Li, X. L. Zhu, X. Q. Liu, and X. M. Chen, Evolution of structure, dielectric properties, and re entrant relaxor behavior in $Ba_5La_xSm_{1-x}Ti_3Nb_7O_{30}$ (x 0.1, 0.25, 0.5) tungsten bronze ceramics. *J. Appl. Phys.* **114**, 044106, (2013).
11. I. Levin, M. C. Stennett, G. C. Miles, D. I. Woodward, A. R. West, and I. M. Reaney, Octahe dral Tilting and Ferroelectric Order in Tetragonal Tungsten Bronze Like Dielectrics. *Appl. Phys. Lett.* **89**, 122908, (2006).
12. M. C. Stennett, I. M. Reaney, G. C. Miles, D. I. Woodward, A. R. West, C. A. Kirk, and I. Levin, Dielectric and structural studies of $Ba_2MTi_2Nb_3O_{15}$ ($BMTNO_{15}$, M Bi^{3+}, La^{3+}, Nd^{3+}, Sm^{3+}, Gd^{3+}) tetragonal tungsten bronze structured ceramics. *J. Appl. Phys.* **101**, 104114, (2007).
13. X. L. Zhu, S. Y. Wu, and X. M. Chen, Dielectric anomalies in $(Ba_xSr_{1-x})_4Nd_2Ti_4Nb_6O_{30}$ ceramics with various radius differences between A1 and A2 site ions. *Appl. Phys. Lett.* **91**, 162906, (2007).
14. X. L. Zhu and X. M. Chen, X. Q. Liu, and X. G. Li, Dielectric relaxations, ultrasonic attenua tion, and their structure dependence in $Sr_4(La_xNd_{1-x})_2Ti_4Nb_6O_{30}$ tungsten bronze ceramics. *J. Mater. Res.* **23**, 3112 3121, (2008).
15. I. Levin, Martin C. Stennett, G. C. Miles, D. I. Woodward, A. R. West, and Ian M. Reaney, Coupling between octahedral tilting and ferroelectric order in tetragonal tungsten bronze struc tured dielectrics. *Appl. Phys. Lett.* **89**, 122908, (2006).
16. X. L. Zhu, X. M. Chen, and X. Q. Liu, Crystal Structure and Dielectric Properties of $Sr_5RTi_3Nb_7O_{30}$ (R La, Nd, Sm, and Eu) Tungsten Bronze Ceramics. *J. Am. Ceram. Soc.* **94**, 1829, (2011).
17. A. A. Bokov, and Z. G. Ye, Recent progress in relaxor ferroelectrics with perovskite structure. *J. Mater. Sci.* **41**, 31 52, (2006).